

Study on **planar segregation** of solute atoms in Mg-Al-Gd alloy system

Xin-Fu Gu^{1,2}, Tadashi Furuhashi², Leng Chen¹, Ping Yang¹

1. School of Materials Science and Engineering, University of Science and Technology Beijing, Beijing, 100083, China
2. Institute for Materials Research, Tohoku University, Sendai, 980-8577, Japan

Abstract

Solute segregation plays an important role in formation of long-period stacking ordered (LPSO) structure in Mg-M-RE (M: Zn, Ni etc., RE: Y, Gd, etc.) alloy systems. In this work, the planar segregation in Mg-Al-Gd alloy is characterized by high angle annular dark field (HAADF) scanning transmission electron microscopy (STEM) and three-dimensional atom probe (3DAP). It is found there is no planar fault accompanying the segregation, and the spatial distribution of segregation may resemble the periodicity of LPSO structure. The segregation is further quantified by 3DAP, and it mainly enriches with Gd atoms. The segregation behaviour is rationalized by First-Principles calculation.

Keywords: Magnesium alloy, Segregation, HAADF-STEM, 3DAP, First-principles

Long-period stacking ordered (LPSO) structures are found to be a new promising strengthening phases for Mg-Zn-RE (RE: rare earth element) alloys, such as Mg-Zn-Y, Mg-Zn-Gd etc. [1-6]. In general, LPSO structure can be found in Mg-M-RE (M: Zn, Cu, Ni, Al, or Co, RE: Y, Gd, Tb, Dy, Ho, Er, Tm) alloy systems [7-11]. The LPSO structure often consists of regular arrangements of four layer height fcc structural units with ABCA stacking sequence (SU for short hereafter) separated by several Mg layers (hcp structure) paralleling to the basal plane (0001)_α, and the SUs usually enrich with RE and M elements [12, 13]. In recent studies, the ideal fcc SU is proposed to contain short-range ordered M₆RE₈ cluster with L₁₂ type structure [10, 13]. Commonly observed LPSO structures 10H, 18R, 14H, and 24R correspond to the

intermediate Mg layers of 1, 2, 3 and 4 layers, respectively [14, 15], where the symbols for the LPSO structures are Ramsdell's notation which specify the total number of $(0001)_\alpha$ layers in the hexagonal unit cell followed by the letter H or R to indicate the lattice type.

A 18R LPSO structure is illustrated in Figure 1(a) viewed from the $[1-210]_\alpha$ direction. 18R contains three fcc SUs in a unit cell, which are highlighted with grey boxes. The SUs enriches with ordered distributed M and RE elements, and the SUs are separated by two Mg layers. The formation of fcc SU is shown in Figure 1(b). The transformation from hcp structure to fcc SU needs two processes. One is the structure change by operating of a partial dislocation of $\langle 1\bar{1}00 \rangle_{\alpha/3}$ type on $(0001)_\alpha$ plane to change the stacking order, and the other is enrichment of M and RE elements by diffusion process. This kind of transformation can be treated as displacive-diffusional transformation process [16-18]. The order of these two processes is the key to understand the formation LPSO structure, and the possible transformation sequences are summarized in Figure 1 in Ref. [19] by Okuda *et al.*. Okuda *et al.* proposed a hierarchical transformation mechanism based on their experimental results by in-situ synchrotron radiation measurements in a melt-quenched amorphous ribbon of Mg-Zn-Y alloy [20]. The solute cluster forms first, subsequently the clusters are spatially arranged accompanying the introduction of stacking faults. However, the formation stage of stacking faults is not directly observed. With the aid of high angle annular dark field (HAADF) scanning transmission electron microscopy (STEM), Kishida *et al.* [21] reported the planar segregation of solute atoms in Mg-Al-Gd for the first time. However, solute atoms Al and Gd are proposed to be co-segregated at this region without direct evidence. Recently, Kim *et al.* [18] found that the co-segregation of Zn and Y atoms forms Guinier-Preston (G.P.) zones in Mg-Zn-Y alloys by using HAADF-STEM and STEM-EDS, and the G.P. zone will transformed to SU by operating of partial dislocation. Matsunaga observed similar phenomenon in Mg-Zn-Gd alloy [22], but the chemical information of G.P. zone is not measured. Nevertheless, the planar segregation seems the precursor phase for formation of LPSO structure. Understanding of composition and structure of the segregation will be

benefit to understand the transformation mechanism of LPSO structure. However, the reported chemical information of segregation is limited. First of all, the atomic species deduced based on the *Z*-contrast method in HAADF-STEM mode should have large difference in atomic number [23], such as RE comparing with other elements in Mg-M-RE alloy, thus it is hard to differentiate two atoms with near atomic number. Secondly, the signal for Energy Dispersive X-ray Spectroscopy (EDS) is weak due to small sample volume and image-drift is another problem during the measurement.

Three-dimensional atom probe (3DAP) tomography could provide three-dimensional maps of chemical heterogeneities in Mg alloy with nano-scale resolution, such as nano-scale precipitates in Mg alloy [24, 25] and clusters of solute atoms [26, 27]. To our knowledge, Inoue *et al.* [28] was the first to apply 3DAP to study the segregation accompanying the well-formed LPSO structures, i.e. at later stage growth of LPSO structure, in Mg-Zn-Y and Mg-Al-Gd alloys. They found only Zn enriched layer on top of 14H LPSO in Mg-Zn-Y alloy, while there is no segregation on top of 18R LPSO. One reason may due to the dynamic feature of the segregation. In Mg-Al-Gd alloy, they conclude the segregation enriches with Gd but is poor at Al, though the Al peak can be clearly seen in their composition profile. Based on these facts, the solute atoms may be not synchronized during LPSO formation. In order to verify this proposal, the early stage of LPSO formation is studied. On one hand, the initial stage of chemical modulation can be studied. On the other hand, one may capture a large number of initial stages to catch the different status of segregation.

The LPSO structure in Mg-Al-Gd alloy shows well-ordered structure [10, 21] and this alloy system is a good candidate to investigate the cluster structure and composition in segregated area. Therefore, the segregation in Mg-Al-Gd alloy will be characterized by STEM and 3DAP techniques in this work, and interaction between solute atoms will be discussed by using first-principles calculation.

Both the as-casted Mg₉₂Al₃Gd₅ alloy (at.% default) and isothermal treated specimen are used in this study. For isothermal treatment, the sample is held at 500°C for 4 hours. TEM specimens of $\phi 3 \times 0.5$ mm were cut from the specimens by using electro-discharge machine. The discs were then mechanically grinded to about 60 μm

and thinned by a dimpling grinder (Model 2000, Fischione) followed by a low-energy ion milling with an voltage varying from 4 kV to 500 V and the incidence angle of 4° (PIPS model 691; Gatan Inc.). The HAADF-STEM observation was carried out with Cs-corrected Titan G2 60-300 (300kV, FEI), and the collection semi-angle of angular detector was 50.5-200 mrad. The 3DAP data was taken by CAMECA LEAP 4000HR at 35 K. A pulse fraction of 20% and a pulse frequency of 200 kHz were applied. The first-principles calculation was carried out with the software named Cambridge Serial Total Energy Package (CASTEP) which implements the plane wave pseudo-potential method of the density functional theory [29]. Electron exchange correlation functional was described by the Perdew-Bruke-Ernzerhof (PBE) version of generalized gradient approximation (GGA) [30]. The tolerance for energy change was set to be 5.0×10^{-6} eV/atom.

Figure 2(a-c) shows some typical atomic-resolution HAADF-STEM images along $[11-20]_\alpha$ and $[01-10]_\alpha$ zone axes in Mg-3Al-5Gd alloy. Figure 2(a, c) shows a single fcc SU with bright contrast in the image. This contrast arises from the enrichment of Gd according to Z-contrast principle [23], because the atomic numbers (Z) for three elements in this study are 12 for Mg, 13 for Al and 64 for Gd, respectively. We can also identify the fcc stacking sequence of SU as indicated as a slash in the image. From the contrast profile shown in the right part of Figure 2(a), apart from the strong peak due to the SU, there are other two peaks (indicated by arrows in the figure) at both top and bottom of the SU. These places should also enrich of solute atoms Gd. In corresponding HAADF-STEM image, they show planar-like segregation spanning several layers, but with hcp structure as in the matrix. There is a solute-deplete zone between the planar segregation and SU. The solute-deplete zone across 2~3 $(0001)_\alpha$ layers. The planar segregation can also be observed at the top 18R LPSO structure as shown in Figure 2(b). These results are consist with the work done by Kishida *et al.* [21]. In order to check whether there are cluster structures in the segregated area, the $\langle 01-10 \rangle_\alpha$ zone axis is selected and the image is shown in Figure 2(c). Within the SU, well-defined clusters can be found at this zone axis, and a single cluster is indicated

by a box. However, contrary to the model of planar segregation [20] and the calculation [31], no obvious ordered cluster is observed in the segregated region. This point was further supported in the aged sample. Figure 3(d-e) shows the 18R LPSO structure after ageing for 4h at 500°C. For 18R LPSO structure, well ordered structure is formed during ageing. A partial transformed SU is indicated by an arrow. The left part has an hcp structure while the right side has an fcc structure. As can be seen from Figure 3(e) at zone axis of $[01-10]_{\alpha}$, the transformed fcc structure has an ordered structure, but the segregated front is not. It seems the segregation helps the formation of planar defects, and the ordered structures only take place after the formation of planar defects.

At the initial stage, the planar segregation could also resemble the periodicity of the LPSO structure as shown in Figure 3(a-c). Several SUs could be observed in this figure, and planar segregations are located between them. After the planar segregation transformed to SU during ageing, it would form a mixed 18R and 14H LPSO, since the interspacing between the SUs are 2~3 $(0001)_{\alpha}$ layers. Figure 3(d) shows the element distribution in this sample measured by 3DAP. The SU enriches both Gd and Al and can be identified. Apart from these contrast for SU, there are some extra segregation in Gd mapping as indicated by arrows. According to the 3D element distribution, the segregation is planar. Furthermore, the composition profile can be generated based on the reconstructed element mapping as shown in the right part of Figure 4(d). Accordingly, Gd content for SU is 9.5~13 at.%, and Al content is about 7-10 at.%. However, for the planar segregated region, Gd content varies from 5-6.5 at.%, while corresponding Al content varies from 1-3 at.%. It is noted that the Al content of about 1 at.% is nearly the same with bulk content, thus there should be no segregation of Al at this composition, such as the planar segregation of Gd at the bottom of element mapping. Therefore, the formation process of LPSO/SU structure could be as follows: Gd atoms firstly segregate, then Al atoms segregate, finally the stacking fault forms accompanying the ordering of Al and Gd to form ordered structure. The finally ordered structure would be similar to Figure 3(e) for aged

sample.

In order to understand the segregation behavior, first-principles calculation is carried out in this study. It seems the planar segregation comes with SU, and the interaction between solute atoms and SU is considered. The calculation model is shown in Figure 4(a). Twelve layers are selected with the SUs located at the bottom and top of the structure. The basal size is selected to be $\sqrt{3}a \times \sqrt{3}a$, where a is the lattice parameter of matrix. During the calculation, the atoms in stacking layer A or C between two SUs are replaced by a solute atom Al or Gd, and total energy is then calculated. Only layers 1~3 in Figure 4(a) are considered due to the mirror symmetry. It is noted that there are different inequivalent sites on each layer. In our model, the inequivalent sites on stacking layer A and C are shown in Figure 4(b) and (c), respectively. There are four inequivalent sites in layer A denoted by A_1 , A_2 , A_3 and A_4 . Three inequivalent sites in layer C are denoted by C_1 , C_2 and C_3 . The convention of these symbols for each inequivalent site is the same as that used by Kishida *et al.*[10, 32]. The calculated results for different positions and layers are shown in Figure 4(d). For simplicity, the total energy has been subtracted by their maximum value for Al or Gd. As for the Gd atoms, the lowest interaction energy with SU is at position A_1 in Layer 2. The second lowest energy position is in Layer 3. It means Gd atoms prefer to be far from the SU. This explains why there is a solute depleted zone between the SU and planar segregation observed by HAADF-STEM. Al has a preferred site C_2 in Layer 1 due to the strong interaction between Al and Gd in the SU. In other positions, Al has almost the same energy. After Gd atoms segregated, Al will segregate in the same area, because Al-Gd has negative binding energy comparing to Al-Al and Gd-Gd pairs [31]. Moreover, Gd segregation can reduce the intrinsic stacking fault energy in $(0001)_\alpha$ plane [33], which can be helpful to form the fcc SU. With the planar defects, the ordered clusters could form as simulated by Kimizuka and Ogata [31].

In summary, the planar segregation in Mg-Al-Gd alloy is characterized by HAADF-STEM and three-dimensional atom probe. The planar segregation often forms together with LPSO structure or its structure units, and the periodic distribution

of segregation resembles the spacing between structure units in LPSO structure. The segregation has an hcp structure, and does not contain obvious cluster structure. The segregation firstly enriches with Gd atoms, and then Al co-segregated due to negative binding energy. The cluster forms accompany the formation of the stacking fault. The segregation behaviour is rationalized by First-Principles calculation.

Acknowledgement

This work was supported by a Grant-in-Aid for Scientific Research on Innovative Areas, "Synchronized Long-Period Stacking Ordered Structure", from the Ministry of Education, Culture, Sports, Science and Technology, Japan (No.23109006) and Fundamental Research Funds for the Central Universities (No. FRF-TP-17-003A1). The Mg alloy used in this study was supplied by Kumamoto University. Special thanks to Mr. Y. Hayasaka for technical support at Electron Microscopy Center, Tohoku University, Japan.

References

- [1] Y. Kawamura, K. Hayashi, A. Inoue, T. Masumoto, *Materials Transactions* 42(7) (2001) 1172-1176.
- [2] Y. Kawamura, T. Kasahara, S. Izumi, M. Yamasaki, *Scripta Materialia* 55(5) (2006) 453-456.
- [3] K. Hagihara, N. Yokotani, Y. Umakoshi, *Intermetallics* 18(2) (2010) 267-276.
- [4] X. Shao, Z. Yang, X. Ma, *Acta Materialia* 58(14) (2010) 4760-4771.
- [5] M. Yamasaki, T. Anan, S. Yoshimoto, Y. Kawamura, *Scripta Materialia* 53(7) (2005) 799-803.
- [6] M. Yamasaki, K. Hashimoto, K. Hagihara, Y. Kawamura, *Acta Materialia* 59(9) (2011) 3646-3658.
- [7] Y. Kawamura, M. Yamasaki, *Materials Transactions* 48(11) (2007) 2986-2992.
- [8] Q.Q. Jin, X.H. Shao, X.B. Hu, Z.Z. Peng, X.L. Ma, *Philos Mag* 97(1) (2017) 1-16.
- [9] S.B. Mi, Q.-Q. Jin, *Scripta Materialia* 68(8) (2013) 635-638.
- [10] H. Yokobayashi, K. Kishida, H. Inui, M. Yamasaki, Y. Kawamura, *Acta Materialia* 59(19) (2011) 7287-7299.
- [11] Z. Luo, S. Zhang, Y. Tang, D. Zhao, *Journal of Alloys and Compounds* 209(1) (1994) 275-278.
- [12] Y.M. Zhu, M. Weyland, A.J. Morton, K. Oh-ishi, K. Hono, J.F. Nie, *Scripta Materialia* 60(11) (2009) 980-983.
- [13] D. Egusa, E. Abe, *Acta Materialia* 60(1) (2013) 166-178.
- [14] E. Abe, A. Ono, T. Itoi, M. Yamasaki, Y. Kawamura, *Philosophical Magazine Letters* 91(10) (2011) 690-696.
- [15] M. Matsuda, S. Ii, Y. Kawamura, Y. Ikuhara, M. Nishida, *Materials Science and Engineering: A* 393(1-2) (2005) 269-274.
- [16] T. Furuhashi, X.F. Gu, *Materials Transactions* 54(5) (2013) 675-679.

- [17] J.F. Nie, Y.M. Zhu, A.J. Morton, *Metallurgical and Materials Transactions A* 45(8) (2014) 3338-3348.
- [18] J.K. Kim, L. Jin, S. Sandlöbes, D. Raabe, *Scientific Reports* (2017) 4046.
- [19] H. Okuda, M. Yamasaki, Y. Kawamura, *Scripta Materialia* 139 (2017) 26-29.
- [20] H. Okuda, M. Yamasaki, Y. Kawamura, M. Tabuchi, H. Kimizuka, Nanoclusters first: a hierarchical phase transformation in a novel Mg alloy, *Scientific Reports*, (2015), 14186.
- [21] K. Kishida, H. Yokobayashi, H. Inui, *Philos Mag* 93(21) (2013) 2826-2846.
- [22] S. Matsunaga, Initial formation stage of long period stacking ordered phase in Mg-based ternary alloys, Graduate School of Engineering, Tohoku University, Sendai, Japan, 2015.
- [23] S.J. Pennycook, D.E. Jesson, *Acta Metallurgica et Materialia* 40(92) (1992) S149–S159.
- [24] D.H. Ping, K. Hono, J.F. Nie, *Scripta Materialia* 48(8) (2003) 1017-1022.
- [25] D.H. Ping, K. Hono, Y. Kawamura, A. Inoue, *Philosophical Magazine Letters* 82(10) (2002) 543-551.
- [26] J.F. Nie, K. Oh-ishi, X. Gao, K. Hono, *Acta Materialia* 56(20) (2008) 6061-6076.
- [27] N. Stanford, G. Sha, A. La Fontaine, M.R. Barnett, S.P. Ringer, *Metallurgical and Materials Transactions A* 40(10) (2009) 2480-2487.
- [28] K. Inoue, N. Ebisawa, T. K., K. Yoshida, K. Nagai, H.X. Xu, D. Egusa, E. Abe, K. Kishida, H. Inui, M. Yamasaki, Y. Kawamura, Analysis of local chemical composition in Mg-TM-RE alloys with LPSO/OD structure by atom probe tomography, International Conference on Magnesium Alloys and Their Applications, Jeju, Korea, 2015.
- [29] S.J. Clark, M.D. Segall, C.J. Pickard, P.J. Hasnip, M.I.J. Probert, K. Refson, M.C. Payne, *Zeitschrift für Kristallographie* 220(5-6) (2005) 567-570.
- [30] J.P. Perdew, K. Burke, M. Ernzerhof, *Physical Review Letters* 77(18) (1996) 3865-3868.
- [31] H. Kimizuka, S. Ogata, *Materials Research Letters* 1(4) (2013) 213-219.
- [32] K. Kishida, H. Yokobayashi, H. Inui, M. Yamasaki, Y. Kawamura, *Intermetallics* 31 (2012) 55-64.
- [33] M. Amitava, K. Seong-Gon, M.F. Horstemeyer, *Journal of Physics: Condensed Matter* 26(44) (2014) 445004.

Figures

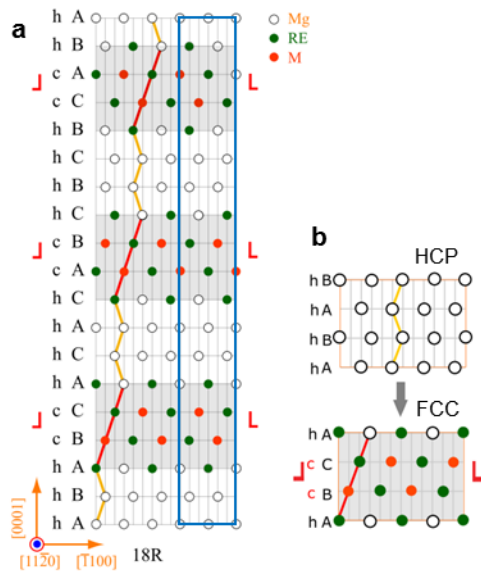


Figure 1. Schematic diagram of 18R LPSO structure viewed along $[11\bar{2}0]_\alpha$ direction. (a) 18R LPSO structure consisting of three fcc structure units separating by two Mg layers. (b) The fcc structure units formed by a shear from the hcp lattice and co-segregation of solute atoms. Each fcc structure unit is highlighted by a grey box.

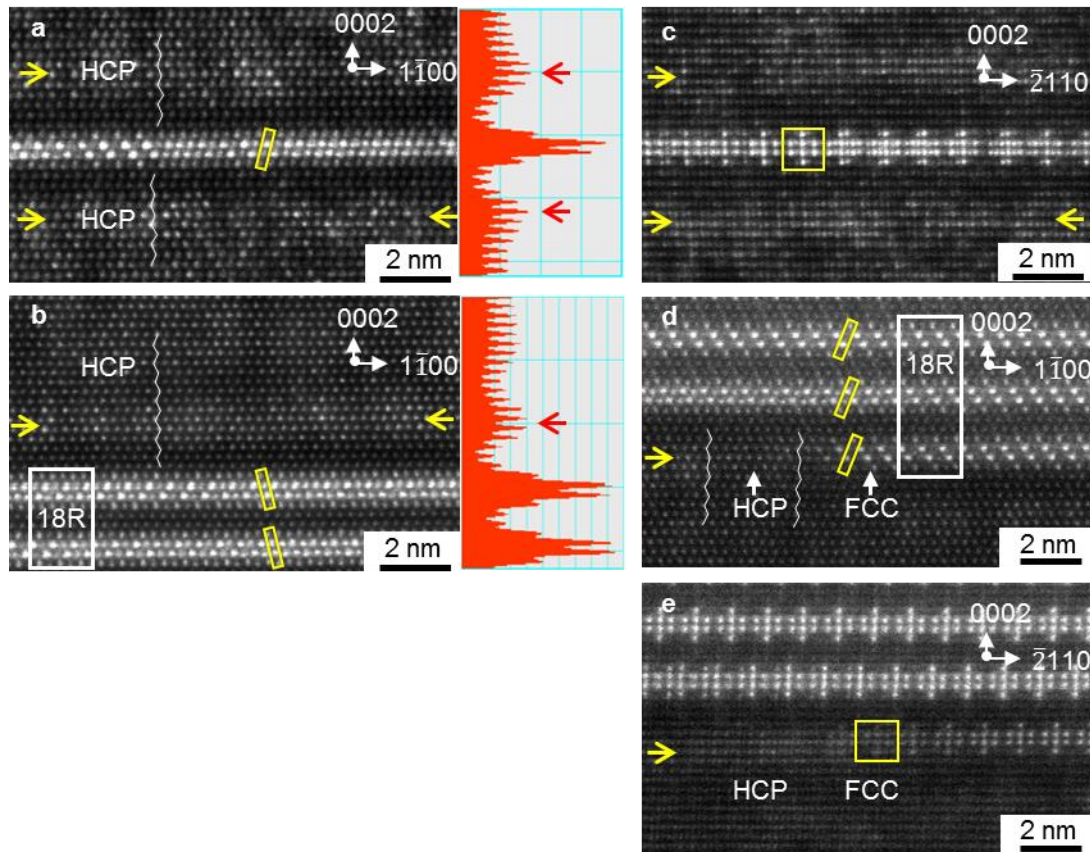


Figure 2. Planar segregation observed by HAADF-STEM. a) segregation around single fcc structure unit in as-casted alloy view along $[11-20]_{\alpha}$, b) segregation during growth of 18R LPSO structure in as-casted alloy viewed along $[11-20]_{\alpha}$. c) view of figure (a) from another direction $[01-10]_{\alpha}$. d) segregation during growth of 18R LPSO structure in the sample aged for 4h at 500°C viewed along $[11-20]_{\alpha}$. e) another zone axis view of figure (d) from $[01-10]_{\alpha}$. The right part of each image shows its corresponding contrast profile. The stacking sequence in fcc structure unit is indicated by a slash. The cluster in the structure units is marked by a yellow box. The arrows indicate the segregation in hcp matrix.

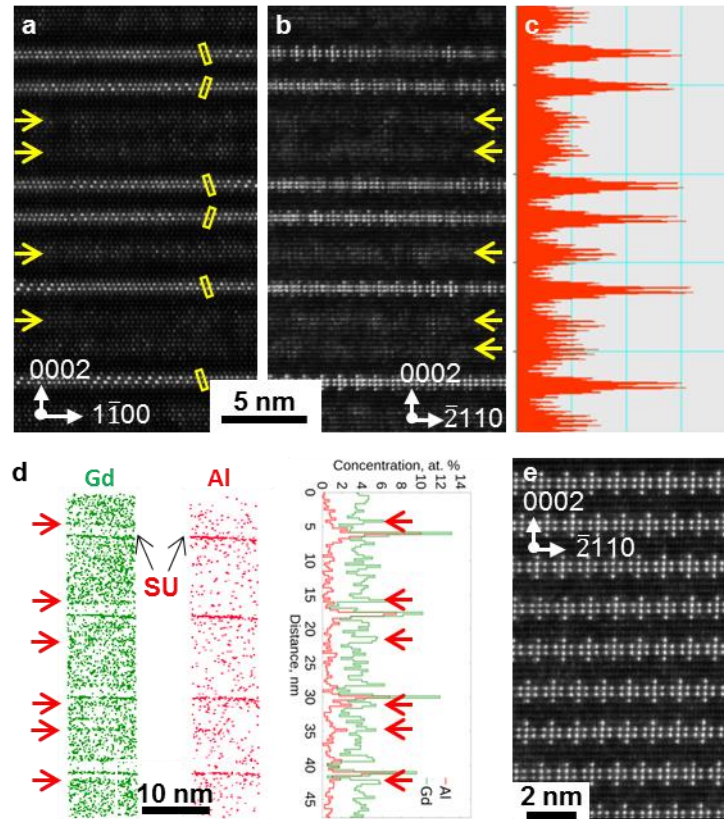


Figure 3. Planar segregation in Mg-Al-Gd alloy. a) HAADF-STEM image of planar segregation in as-casted state viewed along $[11-20]_{\alpha}$ zone axis, b) corresponding image of figure a) viewed along $[01-10]_{\alpha}$ zone axis, c) contrast profile for figure a), d) element mapping of Gd, Al by 3DAP, and their composition profile, e) HAADF-STEM image of 18R LPSO structure after ageing 4h@500°C viewed along $[01-10]_{\alpha}$.

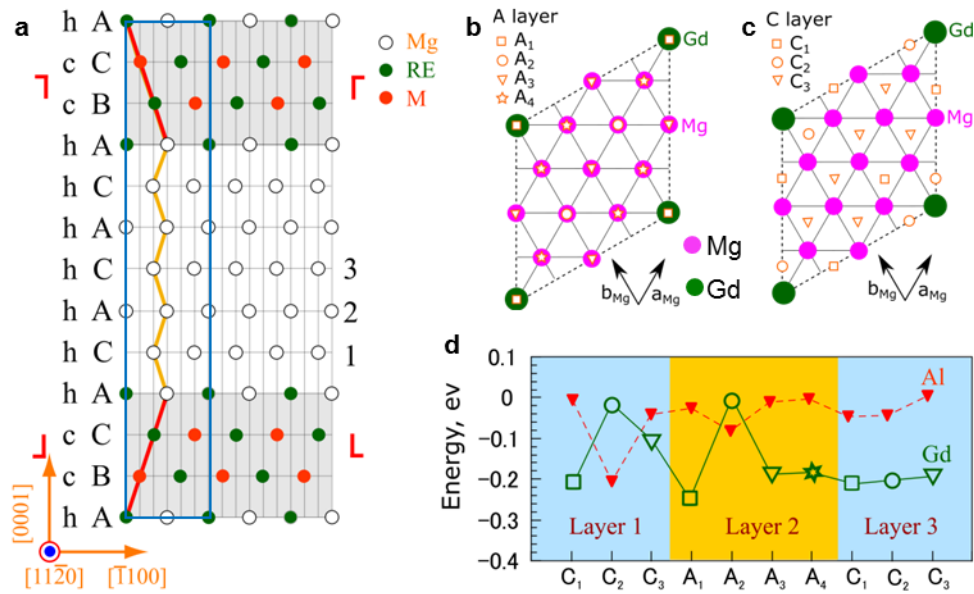


Figure 4. The total energy for the interaction between different solute atoms and SU. a) Schematic diagram of the computational model, the Mg atoms in Layer 1, 2, 3 will be substituted by solute atoms, b) four inequivalent sites on stacking layer A viewed along from $[0001]_a$ direction, c) three inequivalent sites on stacking layer C, d) the energy for Al and Gd in different stacking layers and different positions.